

Going Far Boosts Attack Transferability, but Do Not Do It

Sizhe Chen^{1,2}Qinghua Tao^{1,2}Zhixing Ye^{1,2}Xiaolin Huang*^{1,2}¹Institute of Image Processing and Pattern Recognition, Shanghai Jiao Tong University, China²{sizhe.chen, taoqinghua, yzx1213, xiaolinhuang}@sjtu.edu.cn

Abstract

Deep Neural Networks (DNNs) could be easily fooled by Adversarial Examples (AEs) with an imperceptible difference to original ones in human eyes. Also, the AEs from attacking one surrogate DNN tend to cheat other black-box DNNs as well, i.e., the attack transferability. Existing works reveal that adopting certain optimization algorithms in attack improves transferability, but the underlying reasons have not been thoroughly studied. In this paper, we investigate the impacts of optimization on attack transferability by comprehensive experiments concerning 7 optimization algorithms, 4 surrogates, and 9 black-box models. Through the thorough empirical analysis from three perspectives, we surprisingly find that the varied transferability of AEs from optimization algorithms is strongly related to the corresponding Root Mean Square Error (RMSE) from their original samples. On such a basis, one could simply approach high transferability by attacking until RMSE decreases, which motivates us to propose a LArge RMSE Attack (LARA). Although LARA significantly improves transferability by 20%, it is insufficient to exploit the vulnerability of DNNs, leading to a natural urge that the strength of all attacks should be measured by both the widely used ℓ_∞ bound and the RMSE addressed in this paper, so that tricky enhancement of transferability would be avoided.

1 INTRODUCTION

Deep Learning (DL) has widely served as a mainstream tool in various fields, and its vulnerability has also attracted lots of attention in recent years, among which an apparent instance is the existence of Adversarial Examples (AEs) [Goodfellow et al., 2015, Carlini and Wagner, 2017, Madry

et al., 2018, Tang et al., 2021, Mao et al., 2021]. AEs are slightly perturbed from the natural samples but could cheat *victim* Deep Neural Networks (DNNs) to produce incorrect predictions with high confidence [Szegedy et al., 2014].

Though AEs widely exist, their threat is not very imminent, since attackers generally require sufficient information of the victim DNNs to generate such AEs, i.e., the *white-box attacks*. However, in real-world scenarios, this information (particularly the gradients of the victim) is normally unavailable, and thus one has to perform attacks differently, i.e., the *black-box attacks* [Moosavi-Dezfooli et al., 2017, Cheng et al., 2019, Guo et al., 2019]. One possible approach is to attack a *surrogate* model at hands in white-box manners, and the resulting AEs are expected to have transferability to cheat other unknown victim models, fooling them to predict incorrectly as well, i.e., the *transfer-based attacks*.

Recent works report that adopting a proper optimization algorithm in attacking DNNs, e.g., updating potential AEs with momentum [Dong et al., 2018] or Nesterov acceleration [Lin et al., 2020] gradients from the surrogate may increase the transferability of the crafted AEs. However, the underlying reasons behind the impacts of optimization on attacks are implicit and remain to be explored, i.e.,

“How does optimization influence attack transferability?”

For DNNs, existing analysis on optimization mainly focuses on the training [Kingma and Ba, 2015, Zhuang et al., 2020] rather than their performance in attacks. In this regard, a clear answer to this is fundamental for revealing the mechanism behind high-transferable AEs from an optimization perspective, which is of great significance when developing or introducing optimization algorithms in attacks.

In this paper, we shall answer this question by comprehensive empirical studies involving 7 optimization algorithms, 4 surrogate models, and 9 victim models (including adversarially-trained ones) with diverse architectures. In this way, biases from model architectures can be eliminated to

a significant extent, and then solid results and convincing conclusions are prone to be attained therein.

Based on the performed empirical studies, we find three interesting phenomena that may reveal the answer.

- Optimization algorithms that produce AEs with larger Root Mean Square Error (RMSE) from original samples result in higher-transferable AEs.
- Increasing RMSE of AEs leads to a distinctive boost in transferability when the attack is conducted in an unchanged manner.
- The transferability of AEs from almost all optimization algorithms stays amazingly the same when the RMSE is controlled to a similar value.

Given these observations, we naturally conclude that

“When the ℓ_∞ is controlled, the varied transferability of AEs is strongly related to their varied RMSE.”

RMSE measures the ℓ_2 distance that “*how far do AEs go*”, and is generally considered only in ℓ_2 attack [Carlini and Wagner, 2017] rather than in ℓ_∞ attack. Our conclusion about RMSE is intuitive; see, e.g., Fig. 1, where within a fixed ℓ_∞ bound, an algorithm inducing larger RMSE yields better transferability. The following case is another example under extreme settings: perturbing only one pixel [Su et al., 2019] to the ℓ_∞ bound is surely not good at the transferability, due to the small RMSE.

The conclusion above leads to three further inspirations.

- AEs of Fast Gradient Sign Method (FGSM) transfer better than AEs of Projected Gradient Descend (PGD), owing to the impact of RMSE.
- One could directly attack until RMSE decreases and improve the transferability by over 20% given the large RMSE of AEs, which is our proposed attack strategy, namely the LArge RMSE Attack (LARA).
- We advocate measuring the strength of attack by both ℓ_∞ bound and RMSE under all circumstances because attacks like LARA that merely produce larger RMSE AEs under a fixed ℓ_∞ bound for transferability do not further exploit the vulnerability of DNNs.

We summarize the main contributions of this paper below.

- We study the impacts of optimization on attack transferability by comprehensive experiments concerning 7 algorithms, 4 surrogates, and 9 black-box models.
- We validate from three perspectives that optimization algorithms could increase the transferability by inducing large RMSE between AEs and original samples.
- We highlight the importance of jointly measuring the attack strength by ℓ_∞ bound and RMSE by presenting a simple exemplified high-transferable LARA attack.

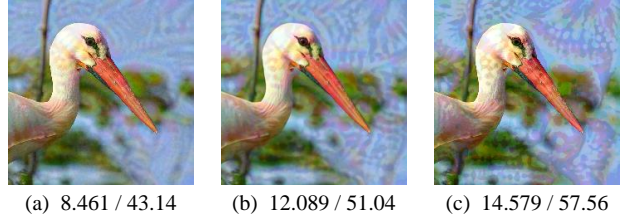


Figure 1: AEs with larger RMSE from original samples tend to have greater transferability. The numbers denote RMSE / average transfer rate. AEs crafted by (a) DI-TI-PGD [Xie et al., 2019b, Dong et al., 2019] do not transfer as good as (b) DI-TI-MI-PGD [Dong et al., 2018] because the former perturbations are significantly covert with a smaller RMSE. Further increasing the RMSE of (b) by our method LARA gets (c), which enjoys the highest transferability. AEs are produced by attacking VGG16 within ℓ_∞ bound 16.

2 RELATED WORK

2.1 ADVERSARIAL ATTACK

In general, the adversarial attack can be described as

$$\begin{aligned} & \text{find } \Delta\mathbf{x}, \\ & \text{s.t. } f(\mathbf{x}) \neq f(\mathbf{x} + \Delta\mathbf{x}), \\ & \quad \|\Delta\mathbf{x}\|_p \leq \varepsilon, \end{aligned} \quad (1)$$

where $f : \Omega \subset \mathbb{R}^n \mapsto y$ refers to the victim model which predicts differently on the original samples $\mathbf{x}_{\text{org}} = \mathbf{x}$ and AEs $\mathbf{x}_{\text{adv}} = \mathbf{x} + \Delta\mathbf{x}$. Here, $\Delta\mathbf{x}$ is the perturbation, which is expected to be imperceptible in human eyes. $\Delta\mathbf{x}$ is commonly restricted by $\|\cdot\|_p$, such as ℓ_1 -, ℓ_2 -, or ℓ_∞ -norm, where ℓ_∞ is the most popular choice.

In training DNNs, a loss function $L(\cdot, \cdot)$ is minimized by updating their parameters $\mathbf{w} \in \mathbb{R}^d$ via gradient descents as

$$\mathbf{w}_{k+1} = \mathbf{w}_k - \Gamma(\nabla_{\mathbf{w}_k} L(f(\mathbf{x}|\mathbf{w}_k), y)), \quad (2)$$

where $\{\mathbf{x}, y\}$ is the training data, and $\Gamma(\cdot)$ represents an optimization algorithm.

Adversarially, attackers maximize the loss function by taking the input \mathbf{x} as the optimized variables, e.g., as follows,

$$\mathbf{x}_{k+1} = \text{clip}_{\mathbf{x}_{\text{org}}}^\varepsilon (\mathbf{x}_k + \Gamma(\nabla_{\mathbf{x}_k} L(f(\mathbf{x}_k|\mathbf{w}), y))), \quad (3)$$

where $\text{clip}(\cdot)$ denotes that the values of \mathbf{x} (e.g., pixels in an image) are clipped to suffice the bounding restriction ε in (1). Such gradient-based attacks [Goodfellow et al., 2015, Madry et al., 2018] are very fast and thereby commonly used [Mao et al., 2021].

2.2 FROM WHITE-BOX TO BLACK-BOX

When the complete knowledge (mostly the gradients) of the victim DNNs is known, attackers are capable of achieving high success rates as described above, among which the PGD [Madry et al., 2018] is recognized as one of the strongest white-box attacks. PGD iteratively updates

$$\mathbf{x}_{k+1} = \text{clip}_{\mathbf{x}_{\text{org}}}^{\epsilon} (\mathbf{x}_k + \alpha \cdot \text{sign}(\nabla_{\mathbf{x}_k} L(f(\mathbf{x}_k | \mathbf{w}), y))),$$

where α is the attack step size, corresponding to the learning rate in typical gradient descent optimization. PGD simply adopts $\Gamma(\cdot) = \alpha \cdot \text{sign}(\cdot)$ but achieves a good success rate.

However, in real-world scenarios, it is commonly impossible to attain the gradient information from the victim model, and thus black-box attacks become essential. In the existing works, black-box attacks either conduct in query-based manners [Cheng et al., 2019, Yang et al., 2020] or with transfer-based approaches [Papernot et al., 2016, 2017]. For the transfer-based methods we concern about in this paper, white-box attacks are carried out on a well-designed surrogate model, and the resulting AEs are expected to cheat other unknown models. To this end, various techniques have been proposed and validated effective in enhancing the attack transferability as described below.

2.3 TRANSFER-BASED ATTACKS VIA OPTIMIZATION

It has been reported that certain optimization algorithms benefit the transferability of AEs. However, besides Momentum (MI, [Dong et al., 2018]) and Nesterov (NI, [Lin et al., 2020]) gradients, other optimization algorithms have not been adopted in attacks to the best of our knowledge. Here, we describe 7 optimization algorithms that could be embedded in adversarial attacks. They are uniformly written as (3), where $\Gamma(\cdot)$ takes the gradients $\mathbf{g}(\mathbf{x}_k)$ as the input, and outputs the optimized direction \mathbf{g}_{k+1} to update as in (4).

In attack, algorithms aim to maximize the loss function $L(\cdot, \cdot)$ by optimizing the variable \mathbf{x} with gradients $\mathbf{g}(\mathbf{x}) = \nabla_{\mathbf{x}} L(f(\mathbf{x} | \mathbf{w}), y)$. To guarantee the imperceptibility (e.g., the pixel-wise RGB restrictions for images), \mathbf{x} is ℓ_{∞} -bounded by threshold ϵ around the original sample \mathbf{x}_{org} as

$$\mathbf{x}_{k+1} = \text{clip}_{\mathbf{x}_{\text{org}}}^{\epsilon} (\mathbf{x}_k + \alpha \cdot \mathbf{g}_{k+1}). \quad (4)$$

Usually, different attacks are restricted to the same ℓ_{∞} bound, for a fair comparison.

Gradient Descent (GD) [Madry et al., 2018]

$$\mathbf{g}_{k+1} = \mathbf{g}(\mathbf{x}_k).$$

Gradient descent algorithm performs the updates through the computed gradient direction. The corresponding attack is one-step FGSM [Goodfellow et al., 2015] and multi-step PGD [Madry et al., 2018].

Momentum Gradient Descent (M-GD) [Dong et al., 2018]

$$\mathbf{g}_{k+1} = \mu \cdot \mathbf{g}_k + \mathbf{g}(\mathbf{x}_k).$$

M-GD accumulates the gradients in a moving-average way, so it implicitly optimizes with more one-stage information as in GD. As a result, it gains a faster convergence and reduces oscillation.

Nesterov Accelerated Gradient Descent (NA-GD) [Lin et al., 2020]

$$\mathbf{g}_{k+1} = \mu \cdot \mathbf{g}_k + \mathbf{g}(\mathbf{x}_k + \alpha \cdot \mu \cdot \mathbf{g}_k).$$

NA-GD makes a big jump in the previously accumulated gradient and does a correction afterward. This predictive strategy prevents it from going too fast and leads to increased responsiveness.

Adam [Kingma and Ba, 2015]

$$\begin{aligned} \mathbf{m}_{k+1} &= \beta_1 \cdot \mathbf{m}_k + (1 - \beta_1) \cdot \mathbf{g}(\mathbf{x}_k), \\ \mathbf{v}_{k+1} &= \beta_2 \cdot \mathbf{v}_k + (1 - \beta_2) \cdot \mathbf{g}^2(\mathbf{x}_k), \\ \mathbf{g}_{k+1} &= \frac{\mathbf{m}_{k+1}}{\sqrt{\mathbf{v}_{k+1}} + \delta}, \end{aligned}$$

where the squared root $\sqrt{(\cdot)}$ is performed element-wisely. Besides storing a moving average of past squared gradients, Adam also keeps that of past gradients as in M-GD. The crucial idea is to go slower in dimensions that have gone far.

L-Adam [Loshchilov and Hutter, 2017]

$$\begin{aligned} \mathbf{m}_{k+1} &= \beta_1 \cdot \mathbf{m}_k + (1 - \beta_1) \cdot (\mathbf{g}(\mathbf{x}_k) - \lambda \cdot \mathbf{x}_k), \\ \mathbf{v}_{k+1} &= \beta_2 \cdot \mathbf{v}_k + (1 - \beta_2) \cdot (\mathbf{g}(\mathbf{x}_k) - \lambda \cdot \mathbf{x}_k)^2, \\ \mathbf{g}_{k+1} &= \frac{\mathbf{m}_{k+1}}{\sqrt{\mathbf{v}_{k+1}} + \delta}. \end{aligned}$$

L-Adam adopts λ to regularize the gradients. The ℓ_2 regularization is very frequently referred to as the weight decay.

AdaBelief [Zhuang et al., 2020]

$$\begin{aligned} \mathbf{m}_{k+1} &= \beta_1 \cdot \mathbf{m}_k + (1 - \beta_1) \cdot \mathbf{g}(\mathbf{x}_k), \\ \mathbf{v}_{k+1} &= \beta_2 \cdot \mathbf{v}_k + (1 - \beta_2) \cdot (\mathbf{g}(\mathbf{x}_k) - \mathbf{m}_{k+1})^2, \\ \mathbf{g}_{k+1} &= \frac{\mathbf{m}_{k+1}}{\sqrt{\mathbf{v}_{k+1}} + \delta}. \end{aligned}$$

Compared to Adam, AdaBelief takes a large step when \mathbf{g}_k is close to \mathbf{m}_k , and a small step when \mathbf{g}_k greatly deviates from \mathbf{m}_k . AdaBelief has better convergence on many tasks with no extra costs.

M-SVAG [Balles and Hennig, 2018]

$$\begin{aligned}\mathbf{m}_{k+1} &= \beta \cdot \mathbf{m}_k + (1 - \beta) \cdot \mathbf{g}(\mathbf{x}_k), \\ \mathbf{v}_{k+1} &= \beta \cdot \mathbf{v}_k + (1 - \beta) \cdot \mathbf{g}^2(\mathbf{x}_k), \\ \rho_{k+1} &= \frac{(1 - \beta)(1 + \beta^{k+2})}{(1 + \beta)(1 - \beta^{k+2})}, \\ \mathbf{g}_{k+1} &= \frac{(1 - \rho_{k+1}) \cdot \mathbf{m}_{k+1}^2}{(1 - 2\rho_{k+1}) \cdot \mathbf{m}_{k+1}^2 + \rho_{k+1} \cdot \mathbf{v}_{k+1}} \cdot \mathbf{m}_{k+1}.\end{aligned}$$

Momentum Stochastic Variance-Adapted Gradient (M-SVAG), compared to M-GD, applies variance adaptation to update the direction. The formula above has been transformed without change.

2.4 OTHER TRANSFER-BASED ATTACKS

Other transfer-enhancement techniques are not our focus in this paper, but we involve them in comparative experiments.

Data Augmentation In [Xie et al., 2019b], the Diverse Input (DI) is proposed to produce AEs using average gradients from randomly-transformed input samples. The Translation Invariant (TI, [Dong et al., 2019]) rather aims to generate AEs with respect to translated copies of the original samples. The Scale Invariant (SI, [Lin et al., 2020]) updates AEs with average gradients from different scale copies of the input.

Specifying Loss Function [Chen et al., 2020] and [Wu et al., 2020] parallelly propose to Attack on Attention (AoA), which aims to suppress the attention heat map along with the cross-entropy. The heat map is a common feature across models, so those attacks boost the transferability.

Specifying Back-Propagation Rules [Wu et al., 2019] exploits the similarity between architectures with residual blocks and attacks by weighted gradients when back-propagating through the residual module. [Guo et al., 2020] proposes to remove the activation function when back-propagating the attack gradients.

3 RMSE IMPACTS TRANSFERABILITY

Although certain optimization algorithms have been reported as effective to improve the transferability when embedded in attacks, the underlying reason remains unexplored. Thus, a comprehensive study towards the impact of optimization on transferability would be necessary and useful for attackers to understand and develop new algorithms.

In this section, we first introduce our overall experimental setup, then present three experimental observations coming from 7 algorithms, 4 surrogates, and 9 victims in the following subsections. All observations support our claim that different optimizers produce AEs with different transferability, generally because the AEs have different RMSE.

3.1 SETUP

In all studies, ImageNet [Deng et al., 2009] validation set with 50K images are used as original samples, following the setting in [Xie et al., 2019b, Lin et al., 2020, Chen et al., 2020]. Keras pre-processing function, central cropping, and resizing (to 224 or 299) are adopted to pre-process the inputs. In all experiments, 1K images are randomly (with a fixed seed) selected and the images falsely predicted by the surrogate model are skipped as in [Su et al., 2018, Chen et al., 2020]. Experiments are implemented in TensorFlow [Abadi et al., 2015], Keras [Chollet et al., 2015] with 4 NVIDIA GeForce RTX 2080Ti GPUs.

For attack and test, several well-trained models in Keras Applications are used. VGG16 [Simonyan and Zisserman, 2015], ResNet50 (RN50) [He et al., 2016], InceptionV3 (IncV3) [Szegedy et al., 2016], and DenseNet121 (DN121) [Huang et al., 2017] are attacked as surrogate models. VGG19 [Simonyan and Zisserman, 2015], ResNet152 (RN152) [He et al., 2016], DenseNet201 (DN201) [Huang et al., 2017], InceptionResNetV2 (IncRN2) [Szegedy et al., 2017], Xception (Xcpt) [Chollet, 2017], and NASNetLarge (NASL) [Zoph et al., 2018] are chosen as black-box victims. To enrich the comparison, we also test on some adversarially-trained (not by our attack) black box models, including InceptionV3adv (A1, [Kurakin et al., 2017]), InceptionResNetV2adv (A2, [Kurakin et al., 2017]), and ResNeXt101den (A3, [Xie et al., 2019a]). The extreme diversity of models eliminates the biases from model architectures to a large extent, contributing to the solid conclusion concerning optimization algorithms and RMSE.

The Attack Success Rate (ASR) is taken as the performance metric, which reflects the transferability and is measured by the average error rate of 9 victim models. Meanwhile, we also care about how large the images are perturbed, which could be measured by RMSE. RMSE calculates the ℓ_2 distance that AEs go away as $dist(\mathbf{x}_{adv}, \mathbf{x}_{org}) = \sqrt{\|\mathbf{x}_{adv} - \mathbf{x}_{org}\|_2^2 / N}$, where $N = H \times W \times C$ is the dimension of the sample.

In this section, to fairly evaluate the transferability of optimization algorithms, the optimization problem of the adversarial attack on the surrogate model is solved to a relatively equal degree with updates presented in Section 2.3. That is to say, the loss of the surrogate on AEs is controlled to a fixed value (such as 0.03 in our experiments if not otherwise stated), of which the methodological details are described in Appendix B with all other hyper-parameters. In the next section, we follow [Dong et al., 2019, Lin et al., 2020] to set $\alpha = 2$ and the number of attack iterations as 10 if not particularly stated. In this way, the attack itself could be compared in the general settings with sign updates. All perturbations are ℓ_∞ -bounded by $\epsilon = 16$ following [Xie et al., 2019b, Dong et al., 2019, Lin et al., 2020].

3.2 TRANSFERABILITY CORRELATES WITH RMSE

We first empirically validate the transferability under the above basic setting. Experimental results are plotted in Fig. 2, where two indices are worth mentioning and comparing, i.e., the ASR (transferability) and the RMSE of AEs generated by the tested 7 optimization algorithms.

Looking at the lines (for transferability) and bars (for RMSE) in the same color simultaneously, one could observe that the transferability has a strong correlation with the RMSE. For the transferability, Adam family outperforms the others, and then M-SVAG follows. More specifically, the resulting transferability is ranked: Adam family > M-SVAG > GD > NA-GD \approx M-GD. For the RMSE, the Adam family also stands out, and the rank is similar: Adam family > GD > M-SVAG > NA-GD \approx M-GD. Among the surveyed optimization algorithms, except for a slight difference concerning GD, this phenomenon holds true for the rest of the algorithms. More notably, this overall trend among optimization algorithms remains stable for all 4 surrogates.

The results above show that when the attack is equally conducted on the surrogate, the ASR (transferability) of a certain optimization algorithm has a strong correlation with the corresponding RMSE between AEs and original samples, indicating that RMSE may be an important factor for the transferability. To further validate this hypothesis, we consider directly intervening in the RMSE and to see the effect on the transferability.

3.3 TRANSFERABILITY WITH LARGER RMSE

If the hypothesis is correct, then by straightforward increasing RMSE while keeping other settings the same, the transferability would be boosted. RMSE can be enlarged in several ways. Here, we offer one possible strategy, which is to add a RMSE item to the original attack loss as the following,

$$L'(f(\mathbf{x}|\mathbf{w}), y) = L(f(\mathbf{x}|\mathbf{w}), y) + \gamma \cdot dist(\mathbf{x}, \mathbf{x}_{org}), \quad (5)$$

where $L(f(\mathbf{x}|\mathbf{w}), y)$ is the standard cross-entropy loss, $dist(\mathbf{x}, \mathbf{x}_{org})$ is the added RMSE between the potential AEs and their corresponding original samples, and the parameter $\gamma > 0$ controls the trade-off between the two terms.

With the modified loss function (5), the influence of RMSE item $dist(\mathbf{x}, \mathbf{x}_{org})$ can now be evaluated in a quantitative way, maintaining the cross-entropy item $L(f(\mathbf{x}|\mathbf{w}), y)$ to a fixed value. Under this setting, we extend the experiment of Fig. 2 by performing the attacks with the modified loss (5) until the cross-entropy item $L(f(\mathbf{x}|\mathbf{w}), y)$ reaches the same level as that in Fig. 2, such that the RMSE is the only factor that varies. We can see from Fig. 3 that a definite boost in transferability (from the full lines copied from Fig. 2 to the dotted lines with (5)) is obtained under all circumstances, validating our hypothesis.

Notice that our claim on RMSE is only applicable to the circumstances where the attack is conducted by optimization on the same loss, e.g., cross-entropy. Random perturbations to enlarge the RMSE do not yield good attack performance as demonstrated in Appendix A. In this regard, our proposed attack LARA is still necessary despite the conclusion here.

3.4 TRANSFERABILITY WITH FIXED RMSE

Besides adding an item to induce a large RMSE, another possible validation is to directly control the RMSE to the same level, which of course would produce a similar ASR if our hypothesis is correct. Because if optimization algorithms influence the transferability via RMSE, then fixing RMSE would definitely eliminate this influence chain, leading to a fixed ASR.

Therefore, we carefully tune the hyper-parameters as specified in Appendix B to maintain AEs to have a similar RMSE $dist(\mathbf{x}, \mathbf{x}_{org})$ by stopping attack when AEs approach a pre-set RMSE value 15 and report the results in Fig. 4. Amazingly, the transferability goes into a similar value for all surrogates and even almost all optimization algorithms. The 4 flat lines indicate that the ASR towards 9 victims is found alike however the specific optimization proceeds. Because the intermediate variable, i.e., the RMSE, is controlled unchangeable, optimization algorithms could hardly impact the transferability, which is revealed and demonstrated by nearly all performed empirical studies.

This encouraging discovery also positively supports our hypothesis that optimization impacts the transferability via RMSE because when the RMSE is not allowed to change, algorithms do not work in boosting the transferability just like the powerless curves failing to oscillate in Fig. 4.

4 FURTHER INSPIRATIONS

Previously, we have empirically validated our hypothesis that RMSE is an important factor for optimization to impact transferability. In this section, we demonstrate that the conclusion is beneficial and inspirational to the community. In the past, we could explain the strange phenomenon that FGSM AEs transfer better than PGD AEs. In the present, the transferability could be directly improved by 20% by exploiting our conclusion. In the future, we advocate a fairer evaluation of the attack strength by both the widely used ℓ_∞ bound and the RMSE addressed in this paper jointly to avoid trivial improvements in the attack transferability.

4.1 FGSM TRANSFERS BETTER THAN PGD

As reported in [Su et al., 2018], one-step FGSM attack [Goodfellow et al., 2015] transfers better than multi-step PGD attack [Madry et al., 2018], which is also found under

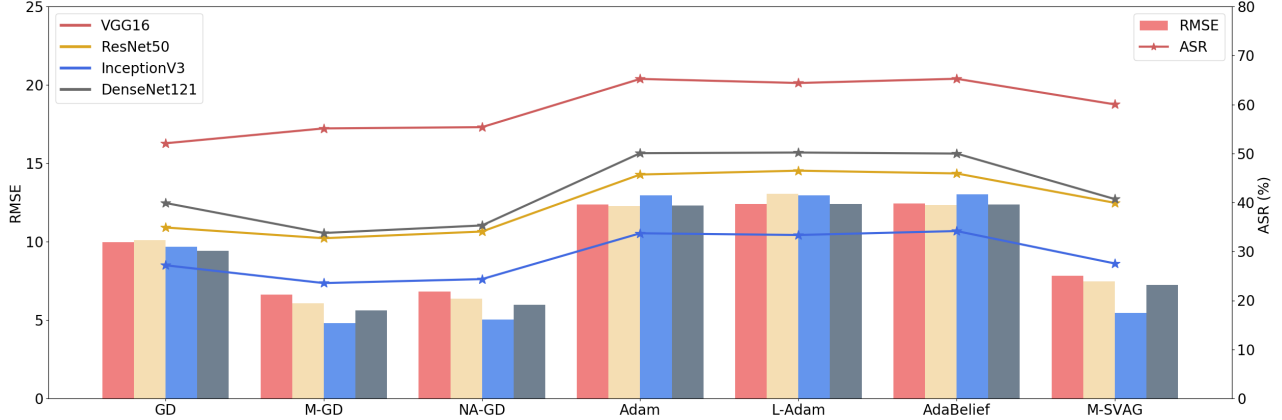


Figure 2: Transferability (lines) and RMSE (bars) of the AEs crafted by 7 optimization algorithms, where the cross-entropy loss of the surrogate model are maintained to 0.03 for fair comparisons. For lines and bars, colors indicate surrogates.

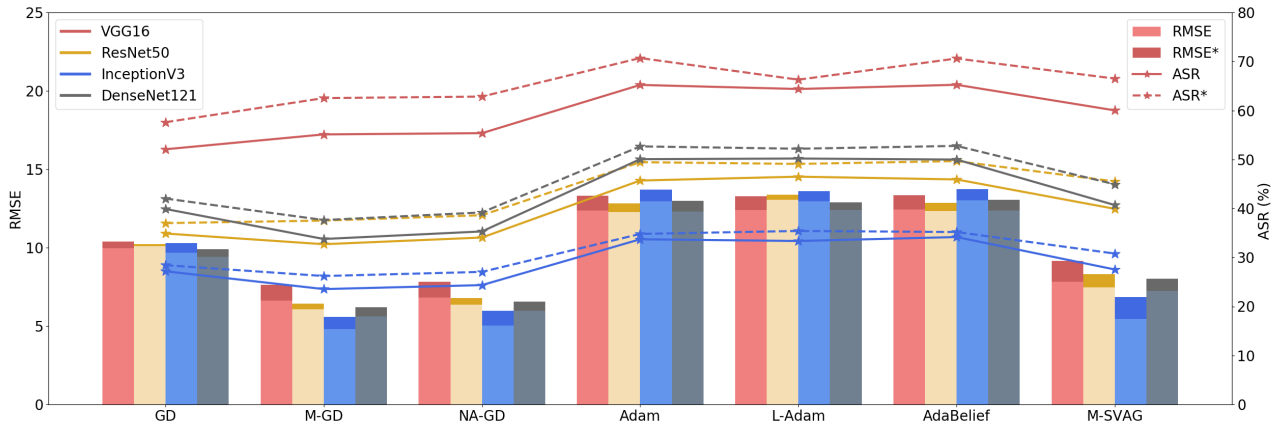


Figure 3: Transferability (lines) and RMSE (bars) of the AEs crafted by 7 optimization algorithms with a constant cross-entropy loss of 0.03 in the surrogates and $\gamma = 0.004$ in the modified loss (5). Full lines and light bars are reference results from Fig. 2. Dotted lines (ASR*) and the shadowed dark bars (RMSE*, on top of the bars) are results with the additional RMSE item in loss, where the AEs reach a larger RMSE when the attack stops at the same cross-entropy loss.

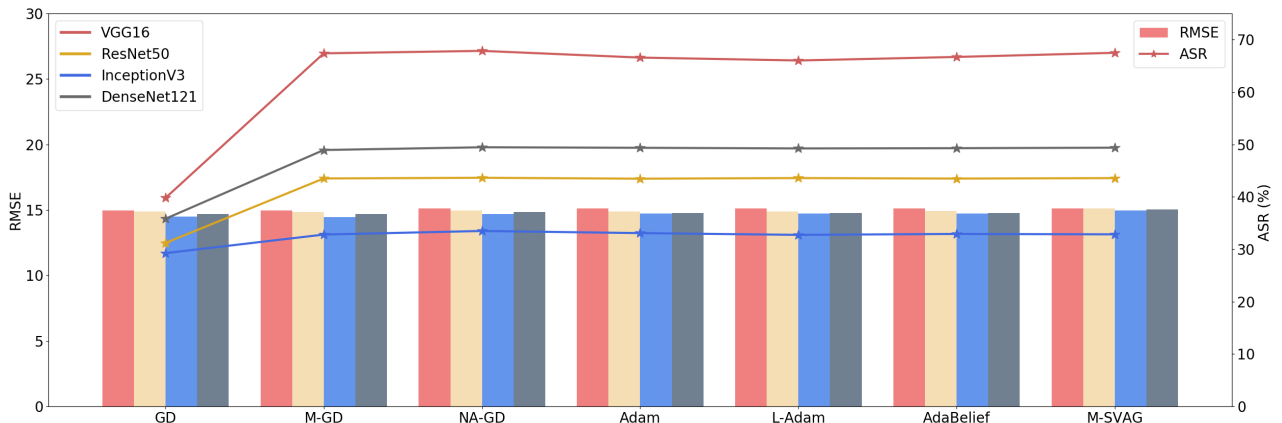


Figure 4: Transferability (lines) and RMSE (bars) of the AEs crafted by 7 optimization algorithms with a constant RMSE, i.e., $dist(\mathbf{x}, \mathbf{x}_{org}) = 15$.



Figure 5: FGSM AE and PGD AE by attacking VGG16 within ℓ_∞ bound 16.

our settings as in reported by Table 1. For three of four surrogates, the ASR of FGSM significantly surpasses PGD. Even for VGG16, the difference in ASR is small. However, this is a bit confusing and contradictory with the common fact that PGD is stronger in white-box settings and produces more diverse patterns, which indicates good transferability to some extent [Chen et al., 2020].

Now based on our conclusion, this phenomenon could be well explained. FGSM perturbs pixels only once, so it extremely exploits the feasible values within the ℓ_∞ bound to push every pixel to the limit, leading to the maximum RMSE. In contrast, PGD iteratively updates the sample with a small step, and the update direction of some pixels are reversed or zero, so they would not reach the limit from ℓ_∞ bound, resulting to smaller RMSE. Numerically, PGD AEs’ RMSE is about $0.4 \times$ that of FGSM as shown in Fig. 1.

FGSM produces AEs with significantly larger RMSE, and the optimization direction is chosen in an insufficiently precise manner, whereas PGD produces diverse adversarial patterns with a small RMSE. However, the brute strategy of FGSM works better mostly, implying that pursuing large RMSE is more important than finding precise optimization direction, in view of the attack transferability.

Table 1: ASR and RMSE of FGSM and PGD

Surrogate	Attack	ASR	RMSE
VGG16	FGSM	58.11	15.57
	PGD	60.34	7.308
RN50	FGSM	43.31	15.56
	PGD	34.60	6.389
IncV3	FGSM	32.02	15.58
	PGD	24.32	6.174
DN121	FGSM	42.02	15.59
	PGD	36.19	6.403

4.2 LARGE RMSE ATTACK (LARA)

It is natural from our conclusion that attackers could generate high-transferable AEs by inducing large RMSE via optimization. In this regard, we propose an exemplified attack strategy, named LArge RMSE Attack (LARA). LARA stops only when RMSE starts to decrease rather than after a certain number of iterations, guaranteeing a greater RMSE to enhance the transferability. LARA is presented in detail in Algorithm 1.

Algorithm 1 LArge RMSE Attack (LARA)

Require: surrogate model f , original sample \mathbf{x}_{org} , label y , ℓ_∞ -norm bound ϵ , attack step size α .
Ensure: adversarial example \mathbf{x}_{adv}

- 1: $\mathbf{x}_0 \leftarrow \mathbf{x}_{\text{org}}$, $k \leftarrow 0$
- 2: $\text{RMSE} \leftarrow 0$, $\text{RMSE_before} \leftarrow 0$
- 3: **while** $\text{RMSE} \geq \text{RMSE_before}$ **do**
- 4: $\text{RMSE_before} = \text{RMSE}$
- 5: $\mathbf{x}_{k+1} = \text{clip}_{\mathbf{x}_{\text{org}}}^{\epsilon} (\mathbf{x}_k + \alpha \cdot \text{sign}(\nabla_{\mathbf{x}_k} L(f(\mathbf{x}_k | \mathbf{w}), y)))$ *
- 6: $\text{RMSE} = \text{dist}(\mathbf{x}_{\text{org}}, \mathbf{x}_{k+1})$
- 7: $k = k + 1$
- 8: **end while**
- 9: **return** \mathbf{x}_k
- 10: * : modified to incorporate DI, TI, SI, MI, AoA.

Comparative experiments on all surrogates and victims are conducted then. According to results in Table 2, LARA boosts the transferability by about 20% compared to baselines. The increase is especially significant when the baseline ASR is low, e.g., Inception-based models as surrogates or victims, which is thus commonly adopted [Dong et al., 2018, Xie et al., 2019b, Dong et al., 2019]. Except for A3 victim, LARA achieves a higher ASR for all tested victims. More results are put in Appendix C.

We visualize the AEs in Fig. 6, from which we find that LARA imposes a stronger attack by inducing larger RMSE. Within the same ℓ_∞ bound, the attack strength could be further improved by continuing the attack and stopping at a proper point, and the transferability would be boosted significantly thereby.

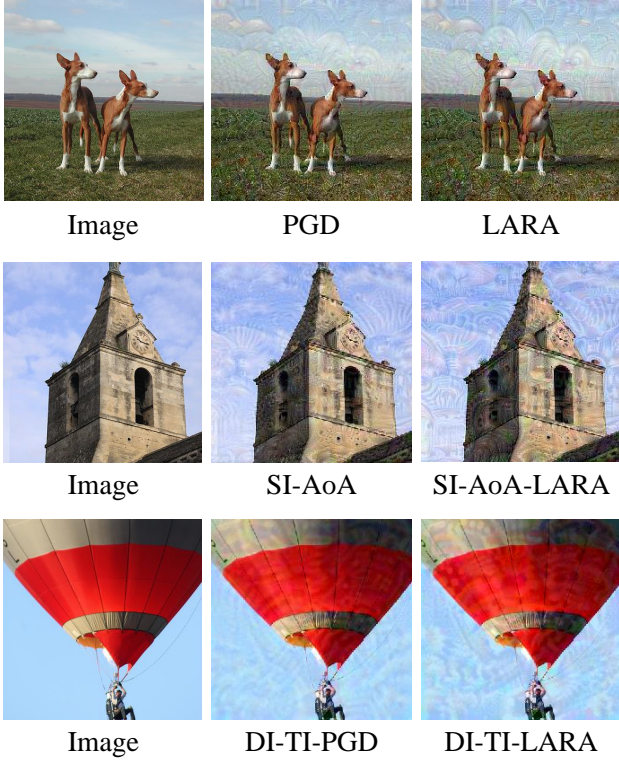
4.3 RMSE MEASURES ATTACK STRENGTH

In most of the current attack experiments, e.g., [Dong et al., 2018, Xie et al., 2019b, Dong et al., 2019, Lin et al., 2020, Mao et al., 2021], the attack strength is measured by $\|\Delta\mathbf{x}\|_\infty$ only. However, as verified in the above experiments, one could change the RMSE to get different attack performance within the same $\|\Delta\mathbf{x}\|_\infty$. In this concern, we advocate measuring the strength of all attacks by both $\|\Delta\mathbf{x}\|_\infty$ and RMSE. In other words, to fairly evaluate the attack transferability, one should maintain the same RMSE under a fixed ℓ_∞ bound in ℓ_∞ attack as in [Chen et al., 2020], and also report the

Table 2: ASR of LARA Compared to Baselines

Surrogate	Attack	Undefended Victim						Adv-Trained Victim		
		DN201	VGG19	RN152	IncRN2	Xcpt	NASL	A1	A2	A3
VGG16	DI-TI-PGD	58.0	91.2	40.7	37.6	44.4	35.1	35.4	29.6	16.3
	DI-TI-LARA	69.9	96.6	48.9	47.6	53.1	50.8	43.9	38.1	17.0
	DI-TI-MI-PGD	67.2	94.8	52.1	47.2	49.3	40.0	47.7	40.9	20.2
	DI-TI-MI-LARA	77.7	98.1	56.7	54.7	60.6	54.1	53.1	45.2	17.8
RN50	DI-TI-PGD	61.4	62.3	42.5	35.2	34.8	30.4	34.3	29.1	17.0
	DI-TI-LARA	72.6	69.9	50.6	43.1	41.0	38.9	40.5	36.9	17.6
	DI-TI-MI-PGD	72.4	74.4	55.6	47.1	48.2	40.0	47.4	40.3	20.7
	DI-TI-MI-LARA	80.1	79.7	60.7	53.4	51.5	45.6	51.8	46.3	20.7
IncV3	DI-TI-PGD	40.4	49.2	38.4	35.8	32.2	22.7	24.3	22.1	22.2
	DI-TI-LARA	49.5	59.2	45.0	45.3	38.7	29.3	32.4	27.9	23.1
	DI-TI-MI-PGD	51.4	62.2	49.3	46.4	43.4	32.7	41.5	35.0	24.2
	DI-TI-MI-LARA	59.2	72.0	54.7	52.7	48.9	38.1	44.4	38.9	24.3
DN121	DI-TI-PGD	75.3	61.9	39.4	36.1	38.6	32.9	29.9	27.6	17.3
	DI-TI-LARA	85.3	71.8	46.4	45.1	47.1	43.7	39.8	35.8	17.4
	DI-TI-MI-PGD	80.7	74.9	51.6	46.7	48.7	42.5	46.8	39.0	21.2
	DI-TI-MI-LARA	92.0	80.7	58.1	56.8	57.8	54.7	54.3	47.2	19.2

RMSE as in [Liu et al., 2017, Wu et al., 2019].

Figure 6: AEs of LARA and baselines. The AEs are crafted by attacking VGG16 [Simonyan and Zisserman, 2015] within ℓ_∞ bound 16.

Conducting a fair test on attack transferability is very important, which could prevent the researchers from explicitly or implicitly resorting to tricky ways to enhance the transferability by enlarging perturbations. With our conclusion and the advocated unprejudiced evaluations, the community should focus on the real vulnerability of DNNs, which is the intentions or meanings of adversarial attacks.

5 CONCLUSION

We in this paper thoroughly investigate the underlying reasons for how optimization algorithms influence the attack transferability. Through the comprehensive experiments involving 7 algorithms, 4 surrogates, and 9 black-boxes, we find that optimization tends to impact the transferability by producing a different RMSE between AEs and original samples. Then, three observations including the transferability under a fixed loss, adding RMSE in attack loss, and the transferability under a fixed RMSE support our hypothesis that optimization algorithms could influence transferability via RMSE. Based on this conclusion, we explain a confusing phenomenon about FGSM and PGD and propose an exemplified method, i.e., LARA, to enhance the transferability by generating large RMSE AEs. However, attacks like LARA to increase RMSE within the same ℓ_∞ bound do not actually exploit the DNN vulnerability, so we advocate measuring the strength of all attacks by ℓ_∞ bound and RMSE jointly.

Acknowledgements

This work was partially supported by National Key Research Development Project (No. 2018AAA0100702, 2019YFB1311503) and National Natural Science Foundation of China (No. 61977046, 61876107, U1803261).

References

Martín Abadi, Ashish Agarwal, Paul Barham, Eugene Brevdo, Zhifeng Chen, Craig Citro, Greg S. Corrado, Andy Davis, Jeffrey Dean, Matthieu Devin, Sanjay Ghemawat, Ian Goodfellow, Andrew Harp, Geoffrey Irving, Michael Isard, Yangqing Jia, Rafal Jozefowicz, Lukasz Kaiser, Manjunath Kudlur, Josh Levenberg, Dandelion Mané, Rajat Monga, Sherry Moore, Derek Murray, Chris Olah, Mike Schuster, Jonathon Shlens, Benoit Steiner, Ilya Sutskever, Kunal Talwar, Paul Tucker, Vincent Vanhoucke, Vijay Vasudevan, Fernanda Viégas, Oriol Vinyals, Pete Warden, Martin Wattenberg, Martin Wicke, Yuan Yu, and Xiaoqiang Zheng. TensorFlow: Large-scale machine learning on heterogeneous systems, 2015. URL <https://www.tensorflow.org/>. Software available from tensorflow.org.

Maksym Andriushchenko, Francesco Croce, Nicolas Flammarion, and Matthias Hein. Square attack: a query-efficient black-box adversarial attack via random search. In *European Conference on Computer Vision*, pages 484–501. Springer, 2020.

Lukas Balles and Philipp Hennig. Dissecting adam: The sign, magnitude and variance of stochastic gradients. In *International Conference on Machine Learning*, pages 404–413. PMLR, 2018.

Nicholas Carlini and David Wagner. Towards evaluating the robustness of neural networks. In *2017 IEEE Symposium on Security and Privacy (SP)*, pages 39–57. IEEE, 2017.

Sizhe Chen, Zhengbao He, Chengjin Sun, and Xiaolin Huang. Universal adversarial attack on attention and the resulting dataset damagenet. In *IEEE Transactions on Pattern Analysis and Machine Intelligence*, 2020.

Shuyu Cheng, Yinpeng Dong, Tianyu Pang, Hang Su, and Jun Zhu. Improving black-box adversarial attacks with a transfer-based prior. In *Advances in Neural Information Processing Systems*, pages 10934–10944, 2019.

François Chollet et al. Keras. <https://keras.io>, 2015.

François Chollet. Xception: Deep learning with depthwise separable convolutions. In *Proceedings of the IEEE Conference on Computer Vision and Pattern Recognition*, pages 1251–1258, 2017.

Jia Deng, Wei Dong, Richard Socher, Li-Jia Li, Kai Li, and Li Fei-Fei. Imagenet: A large-scale hierarchical image database. In *2009 IEEE Conference on Computer Vision and Pattern Recognition*, pages 248–255. IEEE, 2009.

Yinpeng Dong, Fangzhou Liao, Tianyu Pang, Hang Su, Jun Zhu, Xiaolin Hu, and Jianguo Li. Boosting adversarial attacks with momentum. In *Proceedings of the IEEE Conference on Computer Vision and Pattern Recognition*, pages 9185–9193, 2018.

Yinpeng Dong, Tianyu Pang, Hang Su, and Jun Zhu. Evading defenses to transferable adversarial examples by translation-invariant attacks. In *Proceedings of the IEEE Conference on Computer Vision and Pattern Recognition*, pages 4312–4321, 2019.

Ian J Goodfellow, Jonathon Shlens, and Christian Szegedy. Explaining and harnessing adversarial examples. In *STAT*, volume 1050, page 20, 2015.

Yiwen Guo, Ziang Yan, and Changshui Zhang. Subspace attack: Exploiting promising subspaces for query-efficient black-box attacks. In *Advances in Neural Information Processing Systems*, pages 3820–3829, 2019.

Yiwen Guo, Qizhang Li, and Hao Chen. Backpropagating linearly improves transferability of adversarial examples. In *Advances in Neural Information Processing Systems*, 33, 2020.

Kaiming He, Xiangyu Zhang, Shaoqing Ren, and Jian Sun. Deep residual learning for image recognition. In *Proceedings of the IEEE Conference on Computer Vision and Pattern Recognition*, pages 770–778, 2016.

Gao Huang, Zhuang Liu, Laurens van der Maaten, and Kilian Q. Weinberger. Densely connected convolutional networks. In *2017 IEEE Conference on Computer Vision and Pattern Recognition, CVPR*, pages 2261–2269, 2017.

Diederik P. Kingma and Jimmy Ba. Adam: A method for stochastic optimization. In *3rd International Conference on Learning Representations, ICLR*, 2015.

Alexey Kurakin, Ian J. Goodfellow, and Samy Bengio. Adversarial examples in the physical world. In *5th International Conference on Learning Representations, ICLR*, 2017.

Jiadi Lin, Chuanbiao Song, Kun He, Liwei Wang, and John E Hopcroft. Nesterov accelerated gradient and scale invariance for adversarial attacks. In *8th International Conference on Learning Representations, ICLR*, 2020.

Yanpei Liu, Xinyun Chen, Chang Liu, and Dawn Song. Delving into transferable adversarial examples and black-box attacks. In *Proceedings of 5th International Conference on Learning Representations*, 2017.

Ilya Loshchilov and Frank Hutter. Decoupled weight decay regularization. *arXiv preprint arXiv:1711.05101*, 2017.

Aleksander Madry, Aleksandar Makelov, Ludwig Schmidt, Dimitris Tsipras, and Adrian Vladu. Towards deep learning models resistant to adversarial attacks. In *6th International Conference on Learning Representations, ICLR*, 2018.

Xiaofeng Mao, Yuefeng Chen, Shuhui Wang, Hang Su, Yuan He, and Hui Xue. Composite adversarial attacks. In *Proceedings of the Thirty-Fifth AAAI Conference on Artificial Intelligence*, 2021.

Seyed-Mohsen Moosavi-Dezfooli, Alhussein Fawzi, Omar Fawzi, and Pascal Frossard. Universal adversarial perturbations. In *Proceedings of the IEEE Conference on Computer Vision and Pattern Recognition*, pages 1765–1773, 2017.

Nicolas Papernot, Patrick McDaniel, and Ian Goodfellow. Transferability in machine learning: from phenomena to black-box attacks using adversarial samples. *arXiv preprint arXiv:1605.07277*, 2016.

Nicolas Papernot, Patrick McDaniel, Ian Goodfellow, Somesh Jha, Z Berkay Celik, and Ananthram Swami. Practical black-box attacks against machine learning. In *Proceedings of the 2017 ACM on Asia Conference on Computer and Communications Security*, pages 506–519. ACM, 2017.

Karen Simonyan and Andrew Zisserman. Very deep convolutional networks for large-scale image recognition. In *3rd International Conference on Learning Representations, ICLR*, 2015.

Dong Su, Huan Zhang, Hongge Chen, Jinfeng Yi, Pin-Yu Chen, and Yupeng Gao. Is robustness the cost of accuracy?—a comprehensive study on the robustness of 18 deep image classification models. In *Proceedings of the European Conference on Computer Vision (ECCV)*, 2018.

Jiawei Su, Danilo Vasconcellos Vargas, and Kouichi Sakurai. One pixel attack for fooling deep neural networks. In *IEEE Transactions on Evolutionary Computation*. IEEE, 2019.

Christian Szegedy, Wojciech Zaremba, Ilya Sutskever, Joan Bruna, Dumitru Erhan, Ian J. Goodfellow, and Rob Fergus. Intriguing properties of neural networks. In *2nd International Conference on Learning Representations, ICLR*, 2014.

Christian Szegedy, Vincent Vanhoucke, Sergey Ioffe, Jon Shlens, and Zbigniew Wojna. Rethinking the inception architecture for computer vision. In *Proceedings of the IEEE Conference on Computer Vision and Pattern Recognition*, pages 2818–2826, 2016.

Christian Szegedy, Sergey Ioffe, Vincent Vanhoucke, and Alexander A. Alemi. Inception-v4, inception-resnet and the impact of residual connections on learning. In *Proceedings of the Thirty-First AAAI Conference on Artificial Intelligence*, pages 4278–4284, 2017.

Sanli Tang, Xiaolin Huang, Mingjian Chen, Chengjin Sun, and Jie Yang. Adversarial attack type I: Cheat classifiers by significant changes. *IEEE Transactions on Pattern Analysis and Machine Intelligence*, 43(3):1100–1109, 2021.

Dongxian Wu, Yisen Wang, Shutao Xia, James Bailey, and Xingjun Ma. Skip connections matter: On the transferability of adversarial examples generated with resnets. In *7th International Conference on Learning Representations, ICLR*, 2019.

Weibin Wu, Yuxin Su, Xixian Chen, Shenglin Zhao, Irwin King, Michael R Lyu, and Yu-Wing Tai. Boosting the transferability of adversarial samples via attention. In *Proceedings of the IEEE/CVF Conference on Computer Vision and Pattern Recognition*, pages 1161–1170, 2020.

Cihang Xie, Jianyu Wang, Zhishuai Zhang, Yuyin Zhou, Lingxi Xie, and Alan Yuille. Adversarial examples for semantic segmentation and object detection. In *Proceedings of the IEEE International Conference on Computer Vision*, pages 1369–1378, 2017.

Cihang Xie, Yuxin Wu, Laurens van der Maaten, Alan L Yuille, and Kaiming He. Feature denoising for improving adversarial robustness. In *Proceedings of the IEEE Conference on Computer Vision and Pattern Recognition*, pages 501–509, 2019a.

Cihang Xie, Zhishuai Zhang, Yuyin Zhou, Song Bai, Jianyu Wang, Zhou Ren, and Alan L Yuille. Improving transferability of adversarial examples with input diversity. In *Proceedings of the IEEE Conference on Computer Vision and Pattern Recognition*, pages 2730–2739, 2019b.

Jiancheng Yang, Yangzhou Jiang, Xiaoyang Huang, Bingbing Ni, and Chenglong Zhao. Learning black-box attackers with transferable priors and query feedback. *Annual Conference on Neural Information Processing Systems 2020*, 2020.

Juntang Zhuang, Tommy Tang, Sekhar Tatikonda, Nicha Dvornek, Yifan Ding, Xenophon Papademetris, and James S Duncan. Adabelief optimizer: Adapting stepsizes by the belief in observed gradients. *Advances in Neural Information Processing Systems 33: Annual Conference on Neural Information Processing Systems*, 2020.

Barret Zoph, Vijay Vasudevan, Jonathon Shlens, and Quoc V Le. Learning transferable architectures for scalable image recognition. In *Proceedings of the IEEE Conference on Computer Vision and Pattern Recognition*, pages 8697–8710, 2018.

A LARGE RMSE FROM OPTIMIZATION MATTERS

Notably, our emphasis is on the significance of RMSE in how optimization influences transferability. That is to say, a large RMSE is supposed to be induced by optimization rather than random perturbations. We illustrate that by two examples below under the same settings.

Although rescaling the perturbations makes RMSE larger within the same ℓ_∞ bound, it may well not benefit the transferability. We rescale the perturbations from Section 3.2 by M-GD attack to induce a larger RMSE AE $\mathbf{x}'_{\text{adv}} = \text{clip}_{\mathbf{x}_{\text{org}}}^\varepsilon(\mathbf{x}_{\text{org}} + 1.2\Delta\mathbf{x})$, where $\Delta\mathbf{x} = \mathbf{x}_{\text{adv}} - \mathbf{x}_{\text{org}}$. Given the results in Table 3, the large RMSE from rescaling may decrease the ASR.

Table 3: ASR of Rescaled AEs

Surrogate	Attack	ASR	RMSE
VGG16	Original	55.11	6.621
	Rescaled	52.40	7.942
RN50	Original	32.70	6.083
	Rescaled	32.49	7.307
IncV3	Original	23.54	4.804
	Rescaled	25.88	5.768
DN121	Original	33.77	5.616
	Rescaled	34.10	6.734

Further perturbing the pixels far from the ℓ_∞ bound by the random stripes hurts the transferability. Besides rescaling, another strategy to increase RMSE is to particularly handle the “not so perturbed” pixels, i.e., pushing them towards the ℓ_∞ bound manually. Here, we define such pixels as those with a distance less than 15 from the original ones concerning the pixel value. We then replace the perturbations in these pixels with high-transferable random stripes claimed in [Andriushchenko et al., 2020] with $\varepsilon = 16$, then the RMSE would be large. Based on results in Table 4 extended from DI-TI-MI-PGD, we observe a significant drop of ASR resulted from those random perturbations, even the RMSE is large.

B IMPLEMENT DETAILS

Transfer-Based Attacks via Optimization We mostly adopt the hyper-parameters recommended by the proposers. For M-GD, μ is set to 0.9. For Adam, the authors suggest $\beta_1 = 0.9$ and $\beta_2 = 0.999$ as a mild choice. To encourage a fast attack, we eliminate the bias correction term herein. Since \mathbf{g} is extremely smaller than \mathbf{x} in attack, we choose $\lambda = 10^{-12}$ in L-Adam. M-SVAG sets $\beta_1 = \beta_2 = \beta = 0.9$. For Adam family, we select $\delta = 10^{-8}$ to avoid zero division.

Table 4: ASR of AEs with Random Stripe

Surrogate	Attack	ASR	RMSE
VGG16	No Stripe	51.04	12.09
	Stripe	43.63	15.70
RN50	No Stripe	49.57	11.82
	Stripe	43.80	15.69
IncV3	No Stripe	42.90	11.68
	Stripe	39.66	15.69
DN121	No Stripe	50.23	12.10
	Stripe	45.07	15.69

Other Transfer-Based Attacks DI transforms the image for 4 times with probability $p = 1$. The transformation is to resize the image to $0.9 \times$ its size and randomly padding the outer areas with white pixels. SI divides the sample numerically by the power 2 for 4 times. TI adopts a kernel size 15 as suggested. MI uses momentum with $\mu = 1$.

Attack Step The learning rate, or attack step size denoted as α needs to be different for each sample, given the unevenly-distributed gradients across data [Xie et al., 2017]. Accordingly, we need to decide on $\alpha(\mathbf{x})$ to ensure a proper degree of perturbations. Specifically, we make the perturbations after the first attack iteration $\mathbf{x}_1 - \mathbf{x}_0$ have a fixed RMSE ξ as

$$\begin{aligned} & \text{find } \alpha(\mathbf{x}), \\ & \text{s.t. } \mathbf{x}_1 = \text{clip}_{\mathbf{x}_0}^\varepsilon(\mathbf{x}_0 + \alpha(\mathbf{x}_0) \cdot \mathbf{g}_1), \\ & \text{dist}(\mathbf{x}_1, \mathbf{x}_0) = \xi. \end{aligned} \quad (6)$$

Without the sign operation, the optimization direction of algorithms would be precisely preserved in Section 3.

Maintain Loss and RMSE Because the loss and RMSE increase very unstably, we tune ξ for algorithms to achieve a fixed loss or RMSE of the final AEs as specified in Table 5. Attacks stop if the iteration is 10 or the AEs reach the preset loss in Section 3.2, 3.3 and RMSE in Section 3.4.

Table 5: ξ to Maintain Loss or RMSE

Algorithm	Loss	RMSE
GD	0.3	8
M-GD	0.01	2
NI-GD	0.01	2
Adam	1	4
L-Adam	1	4
AdaBelief	1	4
M-SVAG	0.01	2

Table 6: ASR of LARA Compared to Baselines

Surrogate	Attack	Undefended Victim						Adv-Trained Victim		
		DN201	VGG19	RN152	IncRNV2	Xcpt	NASL	A1	A2	A3
VGG16	PGD	80.7	99.1	61.3	63.7	73.1	66.4	45.0	38.1	15.7
	LARA	82.5	99.4	64.3	65.8	74.9	69.0	46.4	39.2	15.7
	SI-AoA	86.9	99.7	73.6	76.2	82.5	73.3	57.2	52.8	18.8
	SI-AoA-LARA	87.9	100.0	79.9	81.4	85.5	81.4	65.0	57.6	15.9
RN50	PGD	65.2	52.3	46.5	34.8	35.9	25.6	19.8	15.9	15.4
	LARA	70.2	56.4	50.0	37.6	39.6	29.1	20.3	16.9	15.7
	SI-AoA	75.4	66.7	65.3	48.1	47.0	35.7	28.2	23.7	15.9
	SI-AoA-LARA	80.4	74.4	66.5	51.9	51.8	40.7	30.2	27.8	16.8
IncV3	PGD	25.1	37.0	26.8	23.8	34.2	20.5	16.4	13.9	21.2
	LARA	28.0	41.4	27.8	25.7	40.6	24.0	17.3	15.4	20.9
	SI-AoA	32.6	43.4	31.0	29.6	44.9	29.1	21.6	17.7	19.8
	SI-AoA-LARA	42.2	49.7	40.7	35.4	52.7	39.0	26.6	24.1	22.0
DN121	PGD	81.6	54.0	40.8	32.0	38.2	29.7	17.3	15.9	16.2
	LARA	89.1	62.8	45.6	38.4	48.4	38.0	20.4	17.5	16.4
	SI-AoA	89.5	66.0	53.6	43.6	47.5	41.7	30.0	25.2	18.1
	SI-AoA-LARA	94.8	75.8	61.9	52.5	57.9	52.2	28.9	25.6	14.4

C MORE RESULTS OF LARA

We report more results of LARA in Table 6. The trend holds that LARA increases ASR towards almost all victims. The RMSE of results in Table 2 and Table 6 is shown in Table 7.

Table 7: RMSE of LARA Compared to Baselines

Surrogate	Attack	RMSE	Attack	RMSE
VGG16	PGD	7.308	DI-TI-MI-PGD	12.08
	LARA	8.064	DI-TI-MI-LARA	14.64
	DI-TI-PGD	8.461	SI-AoA	8.651
	DI-TI-LARA	11.52	SI-AoA-LARA	12.10
RN50	PGD	6.389	DI-TI-MI-PGD	11.82
	LARA	7.815	DI-TI-MI-LARA	14.64
	DI-TI-PGD	7.796	SI-AoA	7.215
	DI-TI-LARA	10.88	SI-AoA-LARA	9.671
IncV3	PGD	6.174	DI-TI-MI-PGD	11.68
	LARA	9.200	DI-TI-MI-LARA	14.27
	DI-TI-PGD	6.786	SI-AoA	6.823
	DI-TI-LARA	10.04	SI-AoA-LARA	10.34
DN121	PGD	6.403	DI-TI-MI-PGD	12.09
	LARA	8.906	DI-TI-MI-LARA	14.59
	DI-TI-PGD	7.497	SI-AoA	7.214
	DI-TI-LARA	10.64	SI-AoA-LARA	11.01